

PAPER • OPEN ACCESS

Optical glass-ceramics based on nanosized crystals of magnesium aluminate spinel doped with iron ions

Recent citations

- [Synthesis, structure and spectroscopy of Fe²⁺:MgAl₂O₄ transparent ceramics and glass-ceramics](#)
Liza Basyrova *et al*

To cite this article: V Bukina *et al* 2020 *J. Phys.: Conf. Ser.* **1697** 012156

View the [article online](#) for updates and enhancements.

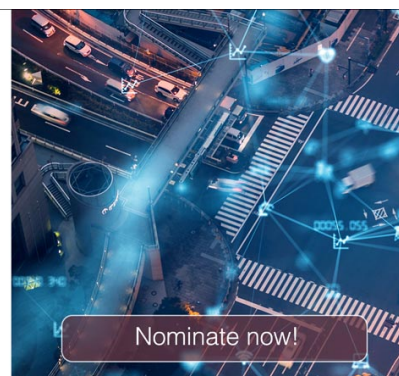


The Electrochemical Society
Advancing solid state & electrochemical science & technology

The ECS is seeking candidates to serve as the
Founding Editor-in-Chief (EIC) of ECS Sensors Plus,
a journal in the process of being launched in 2021

The goal of ECS Sensors Plus, as a one-stop shop journal for sensors, is to advance the fundamental science and understanding of sensors and detection technologies for efficient monitoring and control of industrial processes and the environment, and improving quality of life and human health.

Nomination submission begins: May 18, 2021



Optical glass-ceramics based on nanosized crystals of magnesium aluminate spinel doped with iron ions

V Bukina^{1,*}, O Dymshits^{2,**}, I Alekseeva², M Tsenter², S Zapalova², A Khubetsov², A Zhilin², L Basyrova³, A Volokitina³, J M Serres⁴, X Mateos⁴ and P Loiko⁵

¹ Saint Petersburg Mining University, 2 21st Line Vasil'yevski Ostrov, 199106 Saint Petersburg, Russia

² S.I. Vavilov State Optical Institute, 36 Babushkina St., 192171 St. Petersburg, Russia ³ ITMO University, 49 Kronverkskiy Pr., 197101 Saint-Petersburg, Russia

⁴ Universitat Rovira i Virgili (URV), Física i Cristal·lografia de Materials i Nanomaterials (FiCMA-FiCNA)-EMaS, Marcel·li Domingo 1, 43007 Tarragona, Spain

⁵ Centre de Recherche sur les Ions, les Matériaux et la Photonique (CIMAP), UMR 6252 CEA-CNRS-ENSICAEN, Université de Caen Normandie, 6 Boulevard du Maréchal Juin, 14050 Caen Cedex 4, France

*E-mail: nakara.oriara@mail.ru; **e-mail: vodym1959@gmail.com

Abstract. Transparent glass-ceramics of magnesium aluminum silicate system based on nanosized MgAl_2O_4 spinel crystals nucleated by TiO_2 and doped with Fe_2O_3 were developed. Their structure and spectroscopic properties were studied. The glass-ceramics are important as reference samples in development of saturable absorbers in the short-wave infrared spectral range (2-3 μm).

1. Introduction

Lasers delivering nanosecond (ns) pulses in the short-wave infrared (SWIR) spectral range of 2-3 μm are of practical importance for range finding, remote sensing, meteorology and medical applications. To initiate the pulsed (Q-switched) operation regime in such lasers, ZnS and ZnSe crystals doped with Cr^{2+} and Fe^{2+} ions located in tetrahedral (T_d) sites are used as saturable absorbers [1]. Magnesium aluminate spinel crystals (MgAl_2O_4) with good thermo-mechanical properties are alternative matrices for Fe^{2+} ions [2]. Besides the single crystals and ceramics, MgAl_2O_4 can be obtained in transparent glass-ceramics (GCs). The aim of the present work is to study transparent GCs based on iron-doped MgAl_2O_4 nanocrystals and produced in oxidizing conditions.

2. Experimental

2.1. Synthesis of glass-ceramics

Glass with a composition of 20 MgO , 20 Al_2O_3 , 60 SiO_2 (mol %) nucleated by 10 mol% TiO_2 and doped with 0.05 mol% Fe_2O_3 was melted at 1580 °C with stirring and annealed at 640 °C. To produce transparent and brown-black colored GCs, the glass was subjected to two-stage heat treatments. The nucleation stage was at 750 °C for 6 hours and the crystallization one - at 800 - 1050 °C for 6 hours.



2.2. Structural and spectroscopic studies of glass-ceramics

The X-ray powder diffraction (XRD) patterns of GC samples were recorded using a Shimadzu XRD-6000 diffractometer with Cu K α radiation and a Ni filter. The mean crystal sizes were estimated from broadening of the X-ray peaks according to the Scherrer equation:

$$D_{\text{XRD}} = \frac{K\lambda}{\Delta(2\theta) \cdot \cos\theta}, \quad (1)$$

where λ is the wavelength of the X-ray radiation (1.5406 Å), θ is the diffraction angle, $\Delta(2\theta)$ is the width of the peak at half of its maximum and K is the constant assumed to be 1. The size of spinel crystals was determined using the diffraction peak at $2\theta \approx 65.5^\circ$ and the size of crystals of magnesium aluminotitanate solid solution with a pseudobrookite structure (MAT ss) $x\text{MgTi}_2\text{O}_5 \cdot y\text{Al}_2\text{TiO}_5$ - for the peak at $2\theta \approx 25.7^\circ$. The error for the crystal size estimation was $\sim 5\%$. The microstructure of the samples was studied employing a JEOL TEM-1011 transmission electron microscope (TEM) (acceleration voltage: 100 kV, point resolution: 0.4 nm). The samples were finely powdered and dispersed in ethanol. The TEM images were analyzed with the ImageJ software. All the spectroscopic studies were performed at room temperature (RT, 20 °C). The Raman spectra were measured with the Renishaw inVia confocal Raman microscope using a Leica $\times 50$ objective and an edge filter. The excitation wavelength λ_{exc} was 514 nm (Ar $^+$ ion laser). The absorption spectra of the initial glass and GCs were recorded with a Shimadzu 3600 spectrophotometer in the spectral range 250 - 3300 nm with a resolution of 1 nm. We used plane-parallel polished plates with a thickness of 1 mm.

3. Results

3.1. Structure and phase composition

The initial glass and glass heat-treated at 750 °C for 6 h are X-ray amorphous (Figure 1). This is evidenced by the absence of diffraction peaks and the presence of a typical amorphous halo. After two-stage heat-treatments with a second stage at the temperatures of 800–1000 °C, two crystalline phases, namely MAT ss and MgAl $_2$ O $_4$, crystallize and grow. Sapphirine crystallizes during heat-treatment at 1050 °C, while the material remains transparent.

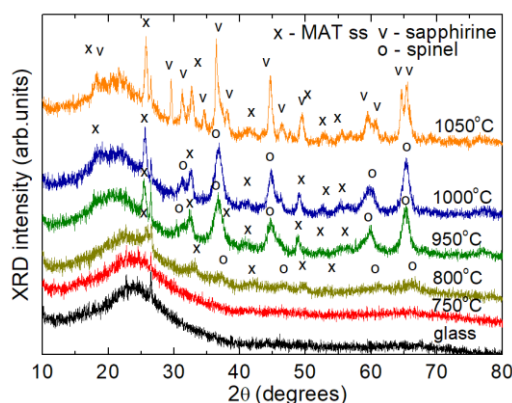


Figure 1. XRD patterns of the initial glass and transparent GCs. Labels 800 – 1050 °C indicate the heat-treatment temperature at the second stage. The nucleation stage is at 750 °C for 6 h.

With an increase in the heat-treatment temperature, the position of the amorphous halo shifts toward that in silica glass and its intensity decreases, which indicates the enrichment of the residual glass with silica caused by formation of spinel and MAT ss. The mean size of the spinel crystals increases with the heat-treatment temperature from 3 to 8 nm, while the size of the MAT ss crystals - from 9 to 14 nm. The value of spinel unit-cell parameter a changes from 7.984 Å to 8.082 Å (Table 1) reflecting a change in the spinel composition from that close to γ -Al $_2$ O $_3$ to a standard MgAl $_2$ O $_4$.

A typical TEM image of the initial glass, Figure 2(a), shows amorphous nearly homogeneous structure. The phase separation develops after the heat-treatment at the nucleation stage, Figure 2(b). In the TEM image of the GC obtained at 950 °C, nanosized crystals are observed. They are most probably the spinel ones.

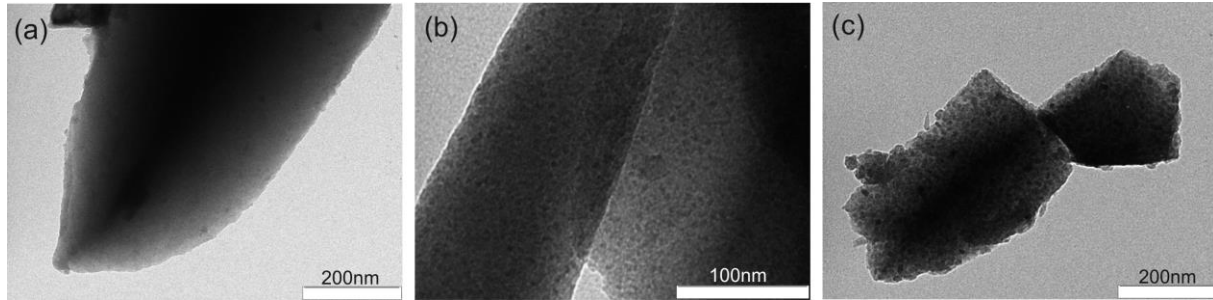


Figure 2. TEM images of (a) the initial glass, (b) glass heat-treated at 750 °C for 6 h, (c) glass heat-treated at 750 °C for 6 h and at 950 °C for 6 h. Please note the different magnification.

3.2. Raman spectra

Raman spectra of the initial and heat-treated glasses, Figure 3(a), demonstrate the structural evolution of the material. The spectrum of the initial glass contains two broad bands, one with a maximum at 480 cm^{-1} and another one of a complex shape with two local maxima at 812 and 919 cm^{-1} . The bands at 480 and 812 cm^{-1} are attributed to vibrations of tetrahedra of the aluminosilicate network. The more intense band at 919 cm^{-1} is associated with vibrations of TiO_4 tetrahedra incorporated into the aluminosilicate network. The spectrum of glass changes after heat-treatment at 750 °C for 6 h (the nucleation stage): the broad band at 480 cm^{-1} shifts to shorter frequencies, 470 cm^{-1} . The band intensities in the high-frequency region are redistributed: the band at 919 cm^{-1} shifts to 904 cm^{-1} and attenuates and the band at 812 cm^{-1} is amplified. These changes are associated with the development of liquid phase separation and formation of the amorphous magnesium aluminotitanate phase wherein titanium ions form TiO_5 and TiO_6 polyhedrons giving rise to a characteristic band at $\sim 800 \text{ cm}^{-1}$ superimposed on the band due to vibrations of tetrahedra of the aluminosilicate network. In the Raman spectrum of GCs obtained at 950 °C, a number of bands appear at 165, 208, 258, 358, 411, 456, 484, 665, 789, and 897 cm^{-1} . All of them except of 411 and 456 cm^{-1} are characteristic of MAT ss [3] and indicate its crystallization from the magnesium aluminotitanate amorphous phase. The band at 411 cm^{-1} is the strongest vibration in the Raman spectrum of magnesium aluminate spinel [4], which is in accordance with the XRD data.

The low-frequency Raman spectra of the initial glass and the glass subjected to heat-treatment at the nucleation stage (at 750 °C for 6 h) did not show certain low-frequency band, Figure 3(b). The distinct band appears after two-stage heat-treatments and its position shifts to lower frequencies with increasing the heat-treatment temperature, Figure 3(b). There is a correlation between the position of the low-frequency Raman band and the size of inhomogeneous regions. The mean size (D_{Raman}) of the inhomogeneous regions is [5]:

$$D_{\text{Raman}} \approx \frac{0.8v_l}{c\nu_{02}^s}. \quad (2)$$

where ν_{02}^s is the frequency of the spheroidal vibration mode corresponding to the low-frequency peak, v_l is the longitudinal velocity of sound in the inhomogeneous regions and c is the speed of light. In our earlier study of phase separation in heat-treated magnesium aluminosilicate glasses nucleated by TiO_2 using small-angle X-ray scattering [6], we demonstrated that a bidispersed system of inhomogeneous regions is formed at initial stages of phase separation. The sizes of the smaller regions were found to be consistent with the sizes obtained from the position of the low-frequency Raman band under an assumption that at the beginning of the process, these are amorphous silicate inhomogeneous regions enriched in magnesium and aluminum, in which spinel crystallizes with increasing the heat-treatment temperature. Large-size inhomogeneous regions, at first also of amorphous nature, form magnesium-

aluminum-titanate phase, from which MAT ss crystallizes with increasing the heat-treatment temperature. The sound velocity for spinel crystals $v_l = 10 \cdot 10^5$ cm/s [3]. When calculating the sizes of inhomogeneous regions D_{Raman} listed in Table 1, we have chosen a slightly lower sound velocity, $v_l = 8 \cdot 10^5$ cm/s, since a certain amount of SiO_2 is always present in magnesium aluminate regions of inhomogeneity. The results in Table 1 allow to conclude that these regions of inhomogeneity are not completely crystallized, since the diameter of spinel crystals according to the XRD and TEM data is approximately half of that calculated from the position of the low-frequency Raman band.

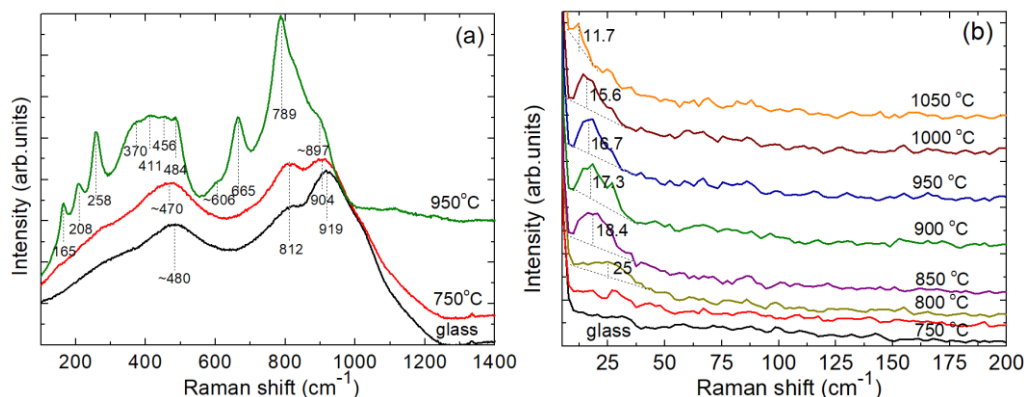


Figure 3. Unpolarized Raman spectra of the initial glass and transparent GCs: (a) the overview in the frequency range of 100-1400 cm^{-1} , (b) a close look on the small-frequency range of 5-200 cm^{-1} with a notch filter. Labels 750 – 1050 $^{\circ}\text{C}$ indicate the heat-treatment temperature at the second stage. $\lambda_{\text{exc}} = 514$ nm, numbers denote the position of the Raman peaks in cm^{-1} .

Table 1. Mean size of nanocrystals D in transparent GCs estimated by different methods* and the unit-cell parameter of spinel nanocrystals a .

Heat-treatment regime	XRD			Raman	TEM
	Spinel		MAT		
	a , Å	D_{XRD} , Å			
	D_{XRD} , Å			D_{Raman} , Å	D_{TEM} , Å
750 °C/6 h	-	-	-	-	23
750 °C/6 h + 800 °C/6 h	7.984	32	85	83	-
750 °C/6 h + 850 °C/6 h	8.028	40	116	88	-
750 °C/6 h + 900 °C/6 h	8.077	57	123	94	-
750 °C/6 h + 950 °C/6 h	8.082	75	128	98	62
750 °C/6 h + 1000 °C/6 h	8.075	82	137	135	-

* D_{XRD} – size determined from the XRD data; D_{Raman} – size determined from low-frequency Raman spectra; D_{TEM} – size determined from the TEM image.

3.3. Optical absorption spectra

The absorption spectra of the initial glass and GCs subjected to two-stage heat-treatments are shown in Figure 4. In all the spectra, the UV absorption band shows the low-energy wing caused by oxygen-to-metal electronic charge transfer transitions $\text{O}^{2-} \rightarrow \text{Ti}^{4+}$, $\text{O}^{2-} \rightarrow \text{Fe}^{2+}$ and $\text{O}^{2-} \rightarrow \text{Fe}^{3+}$. The red-shift of the absorption edge after the heat treatment at 750 $^{\circ}\text{C}$ can be explained by formation of amorphous regions of magnesium aluminum titanate probably containing iron ions. The spectra of the initial glass and glass heat-treated at 750 $^{\circ}\text{C}$ for 6 h contain a weak and broad absorption band spanning from 0.6 to 1.5 μm with a maximum at ~ 1.1 μm , which is associated with Fe^{2+} ions in octahedral (O_h) sites in spinel (the ${}^5\text{T}_2 \rightarrow {}^5\text{E}$ transition). In the absorption spectra, a structureless band with a maximum at ~ 2.8 – 2.9 μm is also observed and attributed to the absorption of OH^- groups.

The absorption spectra of GCs change with increasing the temperature of the secondary stage of heat-treatment in the range of 800–1000 $^{\circ}\text{C}$. A sharp increase in absorption in the visible region is observed,

which may be due to the Fe^{2+} - Fe^{3+} intervalence transition, Fe^{2+} and Fe^{3+} $d \rightarrow d$ transitions in the MAT ss crystals doped with iron ions. A broad band at 1.5–2.5 μm with a maximum at $\sim 1.86 \mu\text{m}$ appears and rises in the spectra of GCs prepared at 850 - 950 $^{\circ}\text{C}$. The increase in the intensity of this band ceases when the heat treatment temperature of the sample reaches 1000 $^{\circ}\text{C}$. This absorption is associated with incorporation of Fe^{2+} ions into spinel nanocrystals in tetrahedral positions (the ${}^5\text{E} \rightarrow {}^5\text{T}_2({}^5\text{D})$ transition). The structuring of the IR absorption band caused by OH^- groups is also connected to spinel crystallization. Indeed, the OH^- groups enter into the spinel structure.

For GC obtained at 1050 $^{\circ}\text{C}$, the absorption band at $\sim 1.86 \mu\text{m}$ decreases, while the absorption at $\sim 1.1 \mu\text{m}$ raises. The position of the UV absorption edge noticeably shifts to $\lambda_{\text{UV}} = 0.38 \mu\text{m}$. All these changes are due to formation of sapphirine at the expense of spinel (see Figure 1).

We believe iron ions are distributed between all precipitated crystalline phases and the residual glass. However, it is extremely difficult to find in absorption spectra traces of the Fe^{2+} and Fe^{3+} ions in the residual silica-rich glass. They are probably concealed within the intense band spreading along the visible and near IR spectral range.

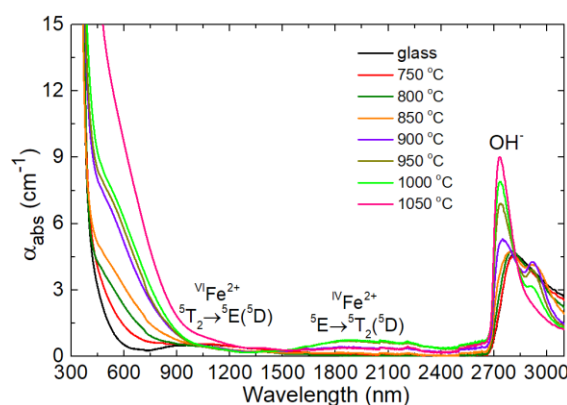


Figure 4. Absorption spectra of the initial glass and transparent GCs. Labels 800 – 1050 $^{\circ}\text{C}$ indicate the heat-treatment temperature at the second stage.

4. Conclusions

Transparent glass-ceramics based on nanosized spinel crystals doped with iron ions were developed. Their structure and phase transformation were studied by XRD, Raman spectroscopy and TEM. In spite of synthesis in oxidizing conditions, a certain part of iron ions added as Fe^{3+} ones are reduced to Fe^{2+} ions during glass melting and heat-treatment. Fe^{2+} ions are located in octahedral and tetrahedral sites in spinel crystals giving rise to broad absorption bands at $\sim 1 \mu\text{m}$ and $\sim 2 \mu\text{m}$, respectively. The developed glass-ceramics are relevant as reference samples for further work on saturable absorbers of lasers emitting at 2-2.3 μm .

Acknowledgments

This work was partly supported by RFBR (Project No. 19-03-00855).

References

- [1] Frolov M P, Korostelin Yu V, Kozlovsky V I, Podmar'kov Yu P, Savinova S A and Skasyrsky Ya K 2015 *Laser Phys. Lett.* **12** 1
- [2] Basyrova L, Balabanov C, Belyaev A, Drobotenko V, Vitkin V, Dymshits O and Loiko P 2019 *J. Phys.: Conf. Ser.* **1410** 012123
- [3] Dymshits O S, A A Zhilin, Petrov V I, Tsenter M Ya, Chuvaeva T I, A V Shashkin, Golubkov V V, Kang U and Lee K H, 2002 *Glass Phys. Chem.* **28** 66
- [4] O'Horo M P, Frisillo A L and White W B, 1973 *J. Phys. Chem. Solids* **34** 23
- [5] Champagnon B, Andrianasolo B and Duval E, 1991 *Mater. Sci. Eng. B* **9** 417

- [6] Golubkov V V, Dymshits O S, Zhilin A A, Chuvaeva T I and Shashkin A V 2003 *Glass Phys. Chem.* **29** 254